

## Exocyclic Delocalization at the Expense of Aromaticity in 3,5-bis( $\pi$ -Donor) Substituted Pyrazolium Ions and Corresponding Cyclic Bent Allenes<sup>†</sup>

Israel Fernández,<sup>‡</sup> C. Adam Dyker,<sup>§</sup> Alan DeHope,<sup>§</sup> Bruno Donnadiou,<sup>§</sup> Gernot Frenking,<sup>\*,||</sup> and Guy Bertrand<sup>\*,§</sup>

*Departamento de Química Orgánica I, Facultad de Ciencias Químicas, Universidad Complutense de Madrid, 28040 Madrid, Spain, UCR-CNRS Joint Research Chemistry Laboratory (UMI 2957), Department of Chemistry, University of California, Riverside, California 92521-0403, and Fachbereich Chemie, Philipps-Universität Marburg, Hans-Meerwein-Strasse, 35032 Marburg, Germany*

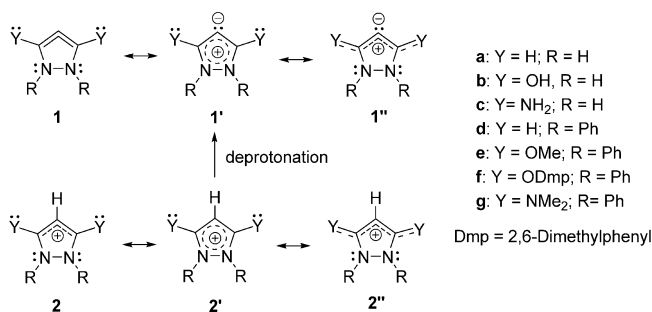
Received April 27, 2009; E-mail: guy.bertrand@ucr.edu; frenking@chemie.uni-marburg.de

**Abstract:** Small ring allenes are usually highly strained and highly reactive species, and for a long time considered only as transient intermediates. The recent isolation of a five membered heterocyclic allene **1f** has raised questions and debate regarding the factors responsible for its stability. Since **1f** has been derived by deprotonation of a pyrazolium ion **2f**, it has been suggested that the stability of **1f** comes from its aromatic character. Here we report computational evidence, including HOMA and NICS aromaticity indices, that allenes derived from 3,5-bis( $\pi$ -donor) substituted pyrazolium salts are weakly aromatic to nonaromatic, and that even their pyrazolium ion precursors have dramatically reduced aromaticity. Exocyclic delocalization, involving the  $\pi$ -donor substituents, occurs at the expense of aromaticity and increases with the strength of the donor. Experimental support for these conclusions is found in the crystallographically determined structure of 3,5-bis(dimethylamino)pyrazolium ion **2g**, which exhibits highly pyramidalized endocyclic nitrogen centers but planarized exocyclic ones, and from the facile C4 protonation to give a stable pyrazole-1,2-dium salt **3g**, which has also been crystallographically characterized.

### Introduction

In the course of our theoretical<sup>1</sup> and experimental<sup>2</sup> work on carbodicarbenes,<sup>3</sup> which can also be regarded as bent allenes, we have recently reported the isolation, and crystallographic characterization of heterocycle **1f** (Scheme 1), which features a CCC bond angle of 97°.<sup>4</sup> Formally, this compound is a five-membered ring allene with two  $\pi$ -donor substituents at each terminus of the allenic fragment, and its thermal stability stands in remarkable contrast to the transient existence of 1,2-cyclopentadiene.<sup>5</sup> Moreover, since the most strained cyclic allenes isolated prior to our work feature angles greater than 156°,<sup>6</sup> the nature of the ground state of **1f** has caused some debate.<sup>7</sup> Because the parent pyrazolium **2a** is recognized as an aromatic heterocycle,<sup>8</sup> and **1f** results from C4-deprotonation of pyrazolium ion **2f**, it has been postulated that the stability of **1f**

**Scheme 1.** Resonance Structures for Allenes **1**, and Their Respective Pyrazolium Ion Precursors **2**



could be due to its aromatic character, as described by resonance from **1f'**. However, we have noted that **1f** features pyramidalized endocyclic nitrogen atoms.<sup>4</sup> This observation suggests that the conjugative interaction of the exocyclic  $\pi$ -donor substituents with the ring, as shown in **1f''**, could be more stabilizing than cyclic electron delocalization within the ring.

Here we report computational and experimental evidence that allenes derived from 3,5-bis( $\pi$ -donor) substituted pyrazolium salts are weakly aromatic to nonaromatic and that even their pyrazolium ion precursors have dramatically reduced aromaticity.

### Results and Discussion

To have a better understanding of the role of the exocyclic  $\pi$ -donor substituents, we chose to theoretically study model

<sup>†</sup> The nonconventional bonding in the compounds derived from deprotonation of pyrazolium ions makes naming them difficult and debatable. Strictly speaking they are not allenes since they do not feature two double bonds from one carbon atom to two others, as defined by IUPAC. (see also Hänninen, M. M.; Peuronen, A.; Heikki, M.; Tuononen, H. M. *Chem. – Eur. J.* **2009**, *15*, 7287–7291) nor are they carbenes [(a) Han, Y.; Huynh, H. V. *Chem. Commun.* **2007**, 1089–1091. (b) Han, Y.; Huynh, H. V.; Tan, G. K. *Organometallics* **2007**, *26*, 6581–6585. (c) Han, Y.; Lee, L. J.; Juyh, H. V. *Organometallics* **2009**, *28*, 2778–2786.] since the central carbon can not be considered as having less than a full octet. These compounds can also be regarded as carbon(0) compounds. For convenience, we will refer to these compounds as cyclic bent allenes.

<sup>‡</sup> Universidad Complutense de Madrid.

<sup>§</sup> University of California.

<sup>||</sup> Philipps-Universität Marburg.

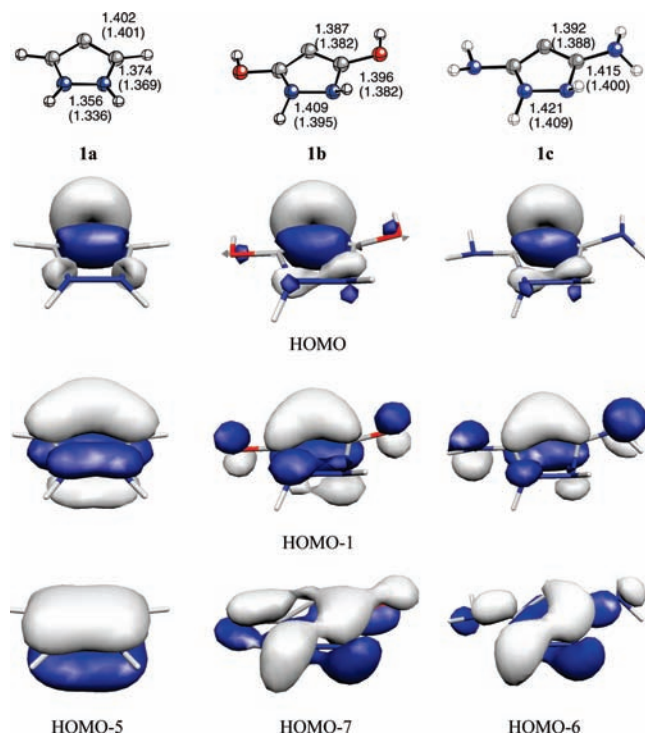


**Figure 1.** Optimized structures (top, BP86/def2-TZVPP and MP2/def2-TZVPP, in parentheses) for **1a**, **1b**, and **1c** (white, gray, red, and blue colors denote hydrogen, carbon, oxygen, and nitrogen atoms, respectively), and their HOMO, HOMO-1, and lowest energy occupied  $\pi$ -type orbitals (HOMO-5, HOMO-7, and HOMO-6, respectively, bottom) computed at the BP86/def2-TZVPP. Bond distances are given in Å.

systems **1a–c**, and experimentally relevant molecules **1d–g**. The optimized (BP86/def2-TZVPP and MP2/def2-TZVPP) structures for **1a–c** are shown in Figure 1 (top), and selected geometric parameters for all allenes **1** are summarized in Table 1, along with crystallographically determined values for compound **1f**. Apparent trends for model compounds **1a–c** are the lengthening of the endocyclic NN and NC bonds, and the increasing bond order of the exocyclic CY bonds, as the donor strength of the substituent increases. Concurrently, the endocyclic nitrogen atoms increasingly pyramidalize, the sum of bond angles going from  $360.0^\circ$  to  $336.8^\circ$  and  $331.1^\circ$  for the parent **1a**, the hydroxyl substituted **1b** and amino substituted **1c**, respectively. It is worth noting that the exocyclic amino groups in **1c** are less pyramidalized (sum of angles =  $344.1^\circ$ ) than the endocyclic ones (computed hybridization:  $sp^{1.75}$  for the exocyclic N atoms and  $sp^{2.01}$  for the endocyclic ones in their respective CN bonds). Moreover, the exocyclic N atoms are engaged in shorter bonds with C3 and C5 than the endocyclic ones, which is also reflected in higher bond orders.

Thus, from a purely structural perspective, it seems that while cyclic electron delocalization, as in Lewis structure **1'**, is prevalent for the parent compound **1a**, the placement of donor substituents in the 3 and 5 positions of the ring favors noncyclic conjugative interactions as in **1''**; not surprisingly, the weight of form **1''** increases with the donor strength of the substituent. The analysis of the occupied  $\pi$ -type orbitals for **1a–c** further supports the conclusion that delocalization involving the exocyclic substituents occurs at the expense of aromaticity. In particular, the lowest lying occupied  $\pi$ -type orbital resembles that of the isoelectronic and aromatic cyclopentadienide in the case of **1a**, but shows significant discontinuity around the ring for **1b**, and even more for **1c** (Figure 1, bottom).

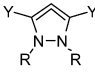
Our calculations (uBP86/def2-TZVPP) indicate that the lowest energy form of the parent 1,2-cyclopentadiene is a biradical singlet state which lies ca. 2.1 kcal/mol below the triplet structure. To see whether a biradical singlet state may also play a role for allenes **1a–c**, we first checked the stability of the BP86 wave functions. The calculations clearly indicate that the BP86 wave function is stable with regard to its spin state. Moreover, we obtained the same optimized structures using the unrestricted uBP86 method with no measurable spin contamination ( $\langle S^2 \rangle = 0.000$ ). Therefore, it is not surprising that the MP2/def2-TZVPP level of theory also leads to quite similar optimized structures (see Figure 1) and to stable wave functions. Furthermore, we also performed a multireferential CASSCF/def2-TZVPP calculation including the  $\pi$ -framework (5 orbitals) and the lone pair orbital at the central carbon atom in the active space for **1a**. The one electron symbolic density matrix which is calculated at the CASSCF level clearly indicates that there is negligible mixing of the configurations which provides further support to the stability of the wave function. Therefore, a multireferential character for compounds **1a–c** similar to the parent 1,2-cyclopentadiene can be safely ruled out. Additionally, we also computed the triplet-singlet gaps for the latter compounds at the BP86/def2-TZVPP level. The computed energy differences ( $\Delta E = 38.9$ , 64.0, and 54.2 kcal/mol for **1a**, **1b**, and **1c**, respectively) show that the situation in the allenes **1a–c** is very different from the parent 1,2-cyclopentadiene.

The theoretical data for **1d–g** suggest that the same conclusion can be drawn as for **1a–c** (Figure 2, Table 1). It is worth noting that the optimized geometry for **1f** agrees quite well with the structure which was determined by X-ray structure analysis.

To gain further insight into the degree of aromaticity in derivatives **1a–g**, we calculated the magnetic (NICS)<sup>9</sup> and geometric (HOMA)<sup>10</sup> aromaticity indices (Table 2). 3,5-Unsubstituted derivatives **1a** and **1d** are predicted to have a high degree of aromaticity by both magnetic and structural criteria, whereas 3,5-bis( $\pi$ -donor) substituted derivatives **1b–c** and **1e–g** demonstrate a significant reduction in aromatic character.

- (1) (a) Tonner, R.; Heydenrych, G.; Frenking, G. *ChemPhysChem* **2008**, *9*, 1474–1481. (b) Tonner, R.; Frenking, G. *Chem.—Eur. J.* **2008**, *14*, 3260–3272. (c) Tonner, R.; Frenking, G. *Chem.—Eur. J.* **2008**, *14*, 3273–3289. (d) Deshmukh, M. M.; Gadre, S. R.; Tonner, R.; Frenking, G. *Phys. Chem. Chem. Phys.* **2008**, *10*, 2298–2301. (e) Tonner, R.; Frenking, G. *Angew. Chem., Int. Ed.* **2007**, *46*, 8695–8698.
- (2) (a) Dyker, C. A.; Lavallo, V.; Donnadiu, B.; Bertrand, G. *Angew. Chem., Int. Ed.* **2008**, *47*, 3206–3209. (b) Melaimi, M.; Parameswaran, P.; Donnadiu, B.; Frenking, G.; Bertrand, G. *Angew. Chem., Int. Ed.* **2009**, *48*, 4792–4795.
- (3) (a) Kaufhold, O.; Hahn, F. E. *Angew. Chem., Int. Ed.* **2008**, *47*, 4057–4061. (b) Fürstner, A.; Alcarazo, M.; Goddard, R.; Lehmann, C. W. *Angew. Chem., Int. Ed.* **2008**, *47*, 3210–3214.
- (4) Lavallo, V.; Dyker, C. A.; Donnadiu, B.; Bertrand, G. *Angew. Chem., Int. Ed.* **2008**, *47*, 5411–5414.
- (5) Daoust, K. J.; Hernandez, S. M.; Konrad, K. M.; Mackie, I. D.; Winstanley, J.; Johnson, R. P. *J. Org. Chem.* **2006**, *71*, 5708–5714.
- (6) (a) Price, J. D.; Johnson, R. P. *Tetrahedron Lett.* **1986**, *27*, 4679–4682. (b) Hofmann, M. A.; Bergstrasser, T.; Reiss, G. J.; Nyulaszi, L.; Regitz, M. *Angew. Chem., Int. Ed.* **2000**, *39*, 1261–1263. (c) Shimizu, T.; Hojo, F.; Ando, W. *J. Am. Chem. Soc.* **1993**, *115*, 3111–3115. (d) Pang, Y.; Petrich, S. A.; Young, V. G.; Gordon, M. S.; Barton, T. J. *J. Am. Chem. Soc.* **1993**, *115*, 2534–2536.
- (7) (a) Christl, M.; Engels, B. *Angew. Chem., Int. Ed.* **2009**, *48*, 1538–1539. (b) Lavallo, V.; Dyker, C. A.; Donnadiu, B.; Bertrand, G. *Angew. Chem., Int. Ed.* **2009**, *48*, 1540–1542.
- (8) (a) Alkorta, I.; Elguero, J. *Tetrahedron* **2006**, *62*, 8683–8686. (b) Kotelevskii, S. I.; Prezhdo, O. V. *Tetrahedron* **2001**, *57*, 5715–5729.
- (9) Schleyer, P. V. R.; Maerker, C.; Dransfeld, A.; Jiao, H. J.; Hommes, N. J. R. *J. Am. Chem. Soc.* **1996**, *118*, 6317–6318.
- (10) (a) Krygowski, T. M. *J. Chem. Inf. Comp. Sci.* **1993**, *33*, 70–78. (b) Cyranski, M. K. *Chem. Rev.* **2005**, *105*, 3773–3811.

**Table 1.** Optimized (BP86/def2-TZVPP) and Crystallographic (Italicized) Structural Parameters for Cyclic Allenes **1**<sup>a</sup>

	C-C [Å] (WBO)	C-N [Å] (WBO)	N-N [Å] (WBO)	C-Y [Å] (WBO)	C-C-C [°]	Σ angles at N [°]	R-N-N-R [°]	C-C-N-N [°]
<b>1a</b> : Y = H, R = H	1.402 (1.51)	1.374 (1.22)	1.356 (1.12)	-	101.1	360.0	0.0	0.0
<b>1b</b> : Y = OH, R = H	1.387 (1.47)	1.396 (1.12)	1.409 (1.04)	1.349 (1.09)	98.4	336.8	86.6	10.3
<b>1c</b> : Y = NH <sub>2</sub> , R = H	1.392 (1.46)	1.415 (1.08)	1.421 (1.03)	1.377 (1.19)	99.6	331.1 (exo = 344.1)	99.7	8.4
<b>1d</b> : Y = H, R = Ph	1.394 (1.51)	1.390 (1.16)	1.373 (1.07)	-	100.7	357.9	27.5	2.7
<b>1e</b> : Y = OMe, R = Ph	1.384 (1.46)	1.407 (1.07)	1.403 (1.02)	1.341 (1.08)	99.7	350.1	59.8	4.1
<b>1f</b> : Y = ODmp, R = Ph	1.382 (1.47)	1.406 (1.07)	1.402 (1.02)	1.350 (1.07)	99.4	350.4	58.9	4.0
<b>1f</b> : <i>X-ray av. values</i> <sup>[a]</sup>	<i>1.378</i>	<i>1.386</i>	<i>1.401</i>	<i>1.352</i>	<i>97.5</i>	<i>349.0</i>	<i>61.5</i>	<i>4.7</i>
<b>1g</b> : Y = NMe <sub>2</sub> , R = Ph	1.390 (1.45)	1.433 (1.01)	1.449 (0.96)	1.366 (1.19)	101.3	335.5 (exo = 359.1)	98.7	0.3

<sup>a</sup> WBO = NBO-Wiberg Bond Order; Dmp = 2,6-dimethylphenyl; [a] Data taken from ref 4.

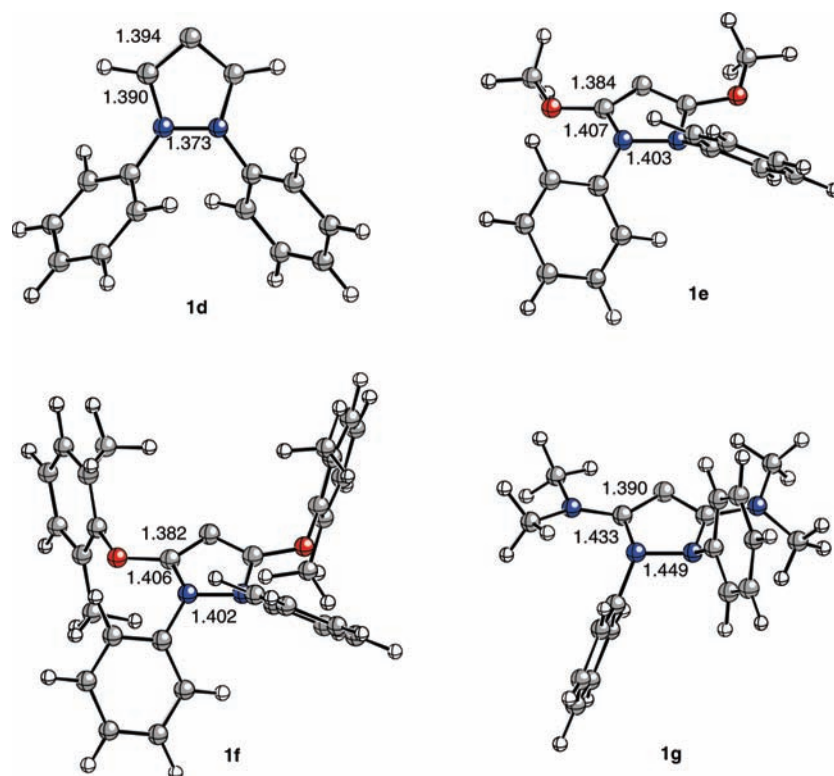


**Figure 2.** Ball and stick representations of the bent allenes **1d–g**. All structures correspond to fully optimized RI-BP/def2-TZVPP geometries. Bond distances are given in Å. White, gray, red, and blue colors denote hydrogen, carbon, oxygen, and nitrogen atoms, respectively.

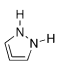
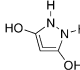
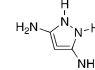
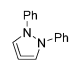
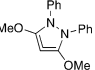
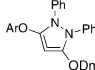
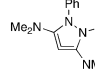
Although the NICS data seem to suggest that **1c** is slightly more aromatic than **1b**, such a quantitative use of NICS values has been cautioned, as their magnitudes do not directly reflect on the relative aromaticity of different systems.<sup>11</sup> Moreover, it can be seen from the calculated HOMA values for model compounds **1a–c** (0.86, 0.60 and 0.43, respectively) that the weight of the form **1'** decreases as the donor ability of the substituents increases. Importantly, NICS and HOMA values calculated at the MP2/def2-TZVPP level show analogous trends and validate the BP86 approach. Of the systems studied, the more experimentally relevant molecules **1e–1g** show the lowest degree of

aromaticity [NICS(1)<sub>zz</sub> and HOMA], and according to the HOMA index (0.12) compound **1g**, which possesses the strongest  $\pi$ -donating NMe<sub>2</sub> groups, is best described as nonaromatic.

Since the aromaticity of derivatives **1** is affected by  $\pi$ -donor substitution, we turned our attention to their conjugate acids **2**. Parameters for the optimized structures of **2a–g** are shown in Table 3 and Figure 3. A comparison of Tables 1 and 3 shows that, upon protonation of a given allene (which according to the HOMOs depicted in Figure 1 occurs in the central carbon atom), there is a widening of the CCC bond angle ( $\Delta_{\text{CCC}} = 5.1–6.6^\circ$ ) and a shortening of both the endocyclic NC bonds ( $\Delta_{\text{NC}} = 0.026–0.044$  Å;  $\Delta_{\text{WBO}} = 0.10–0.15$ ) and, to a lesser degree, the exocyclic CY bonds (Y  $\neq$  H;  $\Delta_{\text{WBO}} = 0.05–0.10$ ).

(11) (a) Gomes, J. A. N. F.; Mallion, R. B. *Chem. Rev.* **2001**, *101*, 1349–1383. (b) Katritzky, A. R.; Jug, K.; Oniciu, D. C. *Chem. Rev.* **2001**, *101*, 1421–1449.

**Table 2.** NICS and HOMA Aromaticity Parameters<sup>a</sup> for Allenes **1**

							
	<b>1a</b>	<b>1b</b>	<b>1c</b>	<b>1d</b>	<b>1e</b>	<b>1f</b>	<b>1g</b>
<b>NICS(0)</b>	-17.50 (-15.40)	-9.00 (-8.85)	-9.86 (-5.75)	-12.84	-9.34	-7.35	-9.52
<b>NICS(1)</b>	-13.13 (-11.73)	-6.14 (-6.39)	-7.64 (-5.56)	-10.19	-6.33	-5.76	-7.09
<b>NICS(1)<sub>zz</sub></b>	-35.14 (-36.02)	-15.32 (-17.33)	-15.80 (-13.48)	-26.09	-11.20	-11.38	-11.25
<b>HOMA</b>	0.86 (0.92)	0.60 (0.72)	0.43 (0.58)	0.77	0.57	0.58	0.12

<sup>a</sup> All data have been computed at the BP86/def2-TZVPP level. Data computed at the MP2/def2-TZVPP level are given in parentheses. Dmp = 2,6-Dimethylphenyl.

**Table 3.** Optimized (BP86/def2-TZVPP) and Crystallographic (Italicized) Structural Parameters for Pyrazolium Ions **2** and Dication **3g**<sup>a</sup>

	C–C [Å] (WBO)	C–N [Å] (WBO)	N–N [Å] (WBO)	C–Y [Å] (WBO)	C–C–C [°]	Σ angles at N [°]	R–N–N–R [°]	C–C–N–N [°]
<b>2a:</b> Y = H, R = H	1.395 (1.46)	1.348 (1.33)	1.352 (1.14)	—	106.2	360.0	0.0	0.0
<b>2a'</b> (pyr)	1.392 (1.46)	1.355 (1.33)	1.391 (1.10)	—	105.8	344.2	74.8	4.1
<b>2b:</b> Y = OH, R = H	1.400 (1.37)	1.362 (1.24)	1.381 (1.07)	1.322 (1.17)	105.0	351.4	53.4	6.7
<b>2c:</b> Y = NH <sub>2</sub> , R = H	1.399 (1.36)	1.382 (1.18)	1.411 (1.04)	1.343 (1.29)	106.1	339.5 (exo = 357.9)	83.2	-8.3
<b>2c'</b> (planar) (ts)	1.404 (1.35)	1.363 (1.22)	1.383 (1.06)	1.348 (1.26)	106.9	360.0	0.0	0.0
<b>2d:</b> Y = H, R = Ph	1.391 (1.45)	1.353 (1.30)	1.380 (1.08)	—	105.8	360.0	3.3	0.2
<b>2e:</b> Y = OMe, R = Ph	1.400 (1.35)	1.363 (1.22)	1.403 (1.02)	1.322 (1.14)	105.0	351.4	25.5	2.2
<b>2f:</b> Y = ODmp, R = Ph	1.397 (1.36)	1.366 (1.21)	1.404 (1.02)	1.326 (1.12)	105.1	357.2	32.1	2.6
<b>2g:</b> Y = NMe <sub>2</sub> , R = Ph	1.402 (1.34)	1.389 (1.15)	1.447 (0.96)	1.346 (1.26)	107.1	344.5 (exo = 358.9)	75.7	3.5
<b>2g:</b> X-ray av. Values <sup>b</sup>	1.392	1.386	1.445	1.332	106.4	339.8 (exo = 358.3)	85.0	4.7
<b>3g:</b> X-ray av. values <sup>b</sup>	1.491	1.341	1.450	1.307	102.6	354.5 (exo = 359.3)	44.4	2.7

<sup>a</sup> WBO = NBO-Wiberg Bond Orders; Dmp = 2,6-dimethylphenyl. <sup>b</sup> See Figure 4.

Within the series of cations **2**, the trends are in line with those observed for allenenes **1**, with NC and NN bonds lengthening, and endocyclic N centers becoming more pyramidalized in the order H < OH < NH<sub>2</sub> (360.0°, 351.4°, 339.5°, computed hybridization: *sp*<sup>2.57</sup>, *sp*<sup>2.61</sup>, and *sp*<sup>2.75</sup>, respectively). It is noted however, that such structural variations occur to a lesser degree in the cation series **2** than in the allene series **1**.

The predicted nonplanarity of the endocyclic nitrogen centers, when donor substituents are present at C3 and C5, prompted us to seek for an experimental confirmation of these unexpected structural features. Cation **2g**<sup>12</sup> was prepared as a tetrafluoroborate salt and single crystals, grown from methanol, were studied by X-ray diffraction (Figure 4, left). The structural parameters (Table 3) are comparable to those predicted theoretically.

In line with expectations based on the structural data, the HOMA index predicts aromaticity to be greater in pyrazolium ions **2** (Table 4) than in the corresponding allenenes **1** (Table 2). This conclusion is not as clear-cut with the NICS calculations (Tables 2 and 4), where in some cases the allene is predicted to be more aromatic by some or all of the magnetic indices. Nevertheless, it remains clear that  $\pi$ -donors in the 3 and 5 positions significantly reduce the aromaticity of both systems **1** and **2** relative to the highly aromatic parent compounds **1a,d** and **2a,d**. Also, the anisotropy of the induced current density (ACID) method,<sup>13</sup> applied to the NH<sub>2</sub> substituted derivative **2c**,

clearly shows that the diatropic current on the ring is affected by the delocalization of the  $\pi$ -lone pairs of the NH<sub>2</sub> groups (Figure 5).

To estimate the contributions of endocyclic nitrogen pyramidalization and exocyclic  $\pi$ -conjugation to the reduced aromatic character of substituted pyrazolium ions, the endocyclic nitrogen environments of **2a** were pyramidalized, whereas those of **2c** were planarized, while allowing all other parameters to be refined without constraint. The optimized structure (Table 3) for the N-pyramidalized derivative **2a'** was found to be a minimum on the potential energy surface, lying 6.8 kcal/mol above planar **2a**. The planarized structure **2c'** was found only as a transition state, 1.7 kcal/mol higher in energy than **2c**. As expected, according to all aromaticity indices (Table 4), **2a'** is clearly less aromatic than the planar global minimum **2a**, but interestingly still more aromatic than **2c**. Again this is a clear indication that the cyclic delocalization is affected by the presence of exocyclic  $\pi$ -donor groups. In a similar way, by all aromaticity indices, planarized **2c'** is found to be more aromatic than nonplanar **2c**, but it is still substantially less aromatic than **2a**. Thus, it can be concluded that the  $\pi$ -type interaction of the exocyclic donor groups with the ring results in a disruption of the electron delocalization within the pyrazolium ring, which is further magnified by the induced pyramidalization of the endocyclic nitrogen atoms. The Second Order Perturbation Theory of the NBO method gives a reasonable explanation of the preference of **2c** (which exhibits exocyclic  $\pi$ -delocalization) over **2c'** (planar-aromatic species). As readily seen in Figure 6, **2c** is clearly favored by a strong stabilizing two-electron interaction between the localized  $\pi$ -lone pair of the central carbon atom and the  $\pi^*$ -C=NH<sub>2</sub> (exocyclic) orbital (associated

(12) Eid, A. I.; Kira, M. A.; Fahmy, H. H. *J. Pharm. Belg.* **1978**, *33*, 303–311.

(13) (a) Geuenich, D.; Hess, K.; Kohler, F.; Herges, R. *Chem. Rev.* **2005**, *105*, 3758–3772. (b) Herges, R.; Geuenich, D. *J. Phys. Chem. A.* **2001**, *105*, 3214–3220.

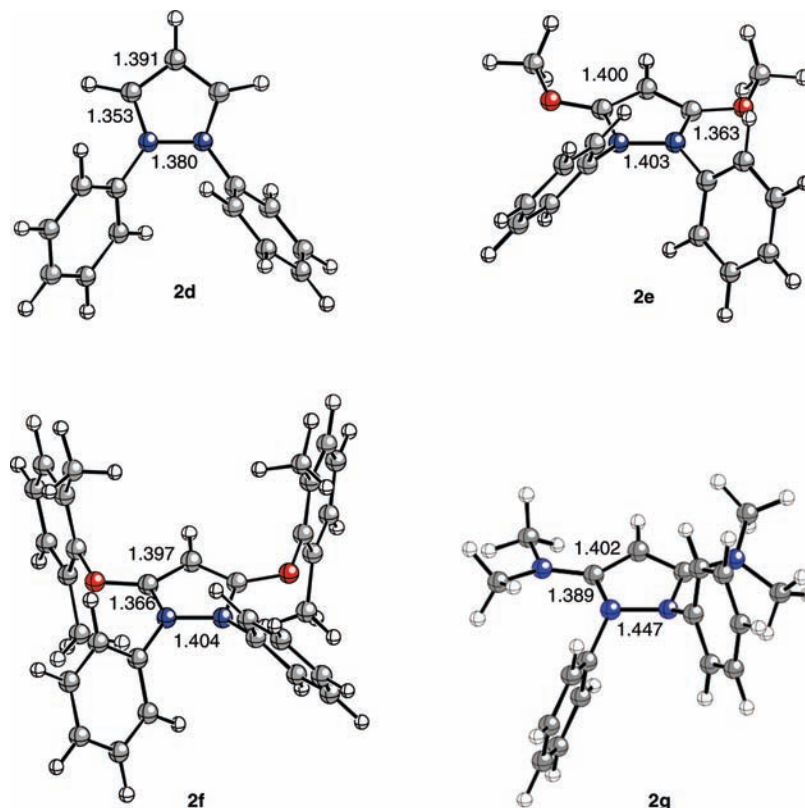


**Figure 3.** Ball and stick representations of the pyrazolium ions **2d**–**g**. All structures correspond to fully optimized RI-BP/def2-TZVPP geometries. Bond distances are given in Å. White, gray, red, and blue colors denote hydrogen, carbon, oxygen, and nitrogen atoms, respectively.

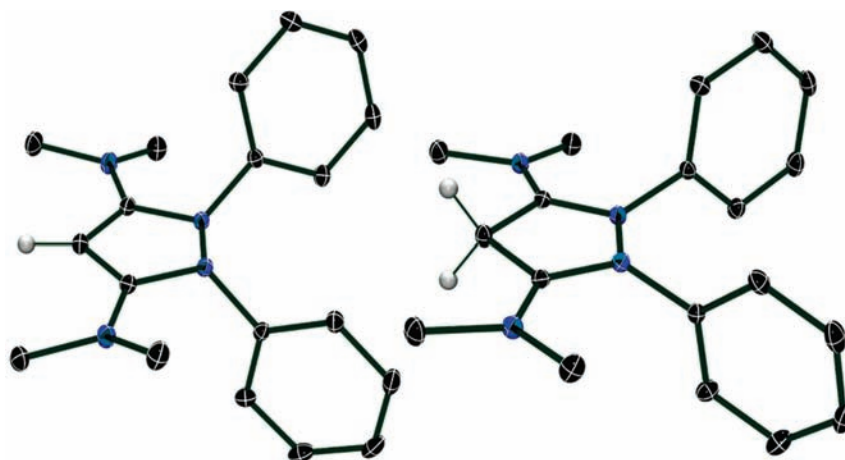


**Figure 4.** Thermal ellipsoid plots (30% probability) of the  $\text{BF}_4^-$  salts of cation **2g** (left) and the dication **3g** (right), with tetrafluoroborate anions and select hydrogen atoms removed for clarity. Averaged structural parameters of interest are given in Table 3. White, black, and blue colors denote hydrogen, carbon, and nitrogen atoms, respectively.

**Table 4.** NICS and HOMA Aromaticity Parameters<sup>a</sup> for Pyrazolium Ions **2**

	2a	2b	2c	2d	2e	2f	2g	2a' (pyr)	2c' (planar)
NICS(0)	−16.37	−12.70	−10.71	−12.24	−11.62	−11.07	−7.92	−12.90	−14.34
NICS(1)	−11.70	−7.33	−5.86	−9.05	−5.55	−5.24	−3.90	−11.88	−6.81
NICS(1) <sub>zz</sub>	−31.86	−17.20	−13.22	−26.80	−15.52	−14.44	−8.73	−29.80	−16.24
HOMA	0.94	0.82	0.63	0.85	0.72	0.72	0.37	0.80	0.80

<sup>a</sup> All data have been computed at the BP86/def2-TZVPP level.

second-order perturbation energy  $\Delta E^{(2)} = -224.9$  kcal/mol). The stabilization from the localized  $\pi$ -lone pair of the exocyclic  $\text{NH}_2$  group to the  $\pi^*$ -C=NH (endocyclic) orbital in **2c'** is reduced to  $-68.6$  kcal/mol. Such a great difference in stabiliza-

tion is very likely the reason for the observed nonplanarity at the expense of a reduced aromaticity.

We find further experimental support for the reduced aromaticity of compound **2g**. Indeed, addition of a slight

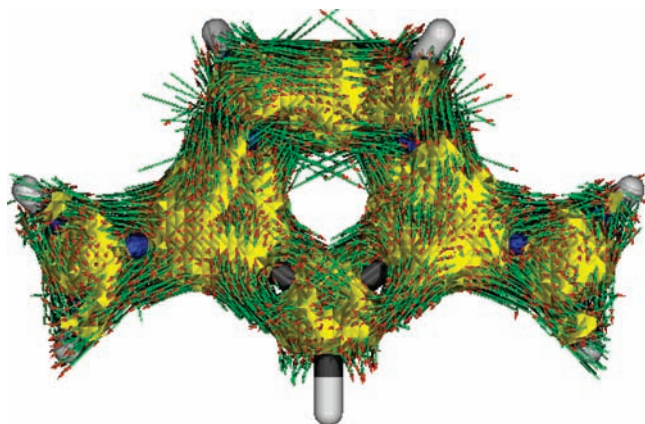


Figure 5. ACID-plot of compound **2c** (isosurface value of 0.05).

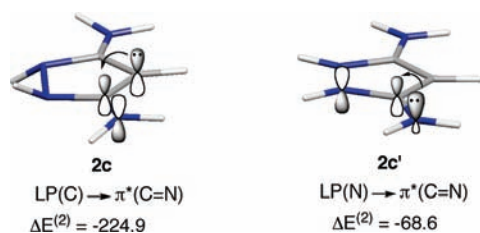
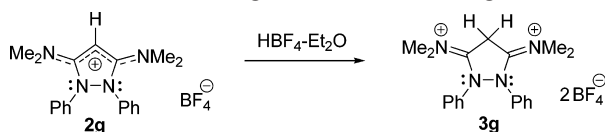


Figure 6. Two-electron interactions and associated second-order perturbation energies,  $\Delta E^{(2)}$  (in kcal/mol) for **2c** and **2c'** cations.

**Scheme 2.** Protonation of **2g**-BF<sub>4</sub> to Give Dication **3g**-2BF<sub>4</sub><sup>a</sup>



<sup>a</sup> Only the dominant resonance structure is drawn for each.

excess of HBF<sub>4</sub>•Et<sub>2</sub>O to an acetonitrile solution of **2g** resulted in the quantitative C4-protonation to form the dication **3g**, as evidenced by <sup>1</sup>H and <sup>13</sup>C NMR spectroscopy, as well as single crystal X-ray crystallography (Figure 4, right; Table 3; Scheme 2). Thus, whereas aniline and even *meta*-phenylenediamine are N-protonated to preserve aromaticity,<sup>14</sup> the preference of C- versus N-protonation in **2g** supports the conclusion that conjugation involving the exocyclic substituents dominates over the cyclic electron delocalization. In dication **3g**, it is again observed that the exocyclic NC bonds (1.307 Å) are shorter than the endocyclic ones (1.341 Å), suggesting the dominance of  $\pi$ -conjugation with the exocyclic amino groups. The endocyclic NC bonds in **3g** are nonetheless shorter than in **2g**, and the NN bonds are statistically identical in the two compounds.

The dramatic structural changes (pyramidalization of the endocyclic nitrogen centers, and lengthening of NC and NN bonds of the ring) and the remarkable loss of aromaticity (showed by HOMA and NICS indices), upon  $\pi$ -donor substitution of the C3 and C5 carbons of **1a** and **2a**, are in stark contrast with observations for the archetypical aromatic molecule benzene. It has been found that both monosubstituted<sup>15</sup> and even

*meta*- and *para*-bis-substituted<sup>16</sup> benzene rings (with various substituents including  $\pi$ -donors such as NH<sub>2</sub> and NMe<sub>2</sub>) show only minor deviations in aromaticity parameters (NICS(1)<sub>zz</sub> values varying by no more than 9.2 ppm and HOMA values between 0.92 and the ideal value of 1.0 for all cases). Only the use of cationic substituents, such as CH<sub>2</sub><sup>+</sup>,<sup>17</sup> or a *para*-substitution pattern involving  $\pi$ -donor and  $\pi$ -acceptor substituents (resulting in a quinoidal ground state) has been observed to reduce the aromaticity of a benzene ring.<sup>10a</sup> The reason  $\pi$ -donors can more easily disrupt the aromaticity of the C<sub>3</sub>N<sub>2</sub> rings of **1** and **2** compared to the benzene ring is likely because the endocyclic nitrogen atoms of the former compounds can more easily accommodate a lone pair of electrons than the endocyclic carbon atoms of the latter. It is remarkable, however that the lone pairs of the amino substituted derivatives of **1** and **2** tend to reside on the endocyclic amino groups rather than the exocyclic ones. Derivatives **1** and **2** represent rare cases where exocyclic delocalization is preferred at the expense of aromaticity, and this results in the unique ability of C3 and C5 amino-substituted pyrazolium salts to be protonated at the C4 carbon, rather than at the exocyclic nitrogen.

### Experimental and Computational Details

All the calculations reported in this paper were obtained with the GAUSSIAN 03<sup>18</sup> and TURBOMOLE<sup>19</sup> suite of programs. The geometries of the molecules were optimized at the gradient corrected DFT level of theory using Becke's exchange functional in conjunction with Perdew's correlation functional (RI-BP86).<sup>20</sup> We used the triple- $\zeta$  basis set denoted by def2-TZVPP which is supposed to be close to the DFT basis set limit.<sup>21</sup> All stationary points were characterized by frequency calculations.<sup>22</sup> Nucleus independent chemical shifts (NICS) were evaluated by using the gauge invariant atomic orbital<sup>23</sup> (GIAO) approach, at the GIAO-BP86/def2-TZVPP//RI-BP86/def2-TZVPP level at the [3,+1] ring critical of the electron density as defined by Bader<sup>24</sup> due to its high sensitivity to diamagnetic effects and its unambiguous character.<sup>25</sup>

The strength of the donor–acceptor orbital interactions have been computed using the natural bond orbital (NBO) method.<sup>26</sup> The

(14) (a) Anderson, K. M.; Goeta, A. E.; Hancock, K. S. B.; Steed, J. W. *Chem. Commun.* **2006**, 2138–2140. (b) Anderson, K. M.; Goeta, A. E.; Hancock, K. S. B.; Steed, J. W. *Chem. Commun.* **2006**, 2722–2722. (c) Kapoor, I. P. S.; Srivastava, P.; Singh, G. *Indian J. Chem. A.* **2007**, *46*, 1277–1282.

(15) (a) Krygowski, T. M.; Stepien, B. T. *Pol. J. Chem.* **2004**, *78*, 2213–2217. (b) Krygowski, T. M.; Ejsmont, K.; Stepien, B. T.; Cyranski, M. K.; Poater, J.; Sola, M. *J. Org. Chem.* **2004**, *69*, 6634–6640. (16) Krygowski, T. M.; Dobrowolski, M. A.; Zborowski, K.; Cyranski, M. K. *J. Phys. Org. Chem.* **2006**, *19*, 889–895. (17) Krygowski, T. M.; Wisiorowski, M.; Nakata, K.; Fujio, M.; Tsuno, Y. *Bull. Chem. Soc. Jpn.* **1996**, *69*, 2275–2279. (18) Frisch, M. J.; et al. *Gaussian 03*, revision E.01; Gaussian, Inc.: Wallingford, CT, 2004. (19) *TURBOMOLE 5.9*, [http://www.cosmologic.de/QuantumChemistry/main\\_turbomole.html](http://www.cosmologic.de/QuantumChemistry/main_turbomole.html). (20) (a) Becke, A. D. *Phys. Rev. A* **1988**, *38*, 3098–3100. (b) Perdew, J. P. *Phys. Rev. B* **1986**, *33*, 8822–8824. (c) Eichkorn, K.; Treutler, O.; Ohm, H.; Haser, M.; Ahlrichs, R. *Chem. Phys. Lett.* **1995**, *242*, 652–660. (21) Weigend, F.; Ahlrichs, R. *Phys. Chem. Chem. Phys.* **2005**, *7*, 3297–3305. (22) McIver, J. W.; Komornicki, A. *J. Am. Chem. Soc.* **1972**, *94*, 2625–2633. (23) Wolinski, K.; Hinton, J. F.; Pulay, P. *J. Am. Chem. Soc.* **1990**, *112*, 8251–8260. (24) Bader, R. F. W. *Atoms in Molecules-A Quantum Theory*; Clarendon Press: Oxford, 1990; pp 12–52. (25) Some examples. (a) Fernández, I.; Sierra, M. A.; Cossío, F. P. *J. Org. Chem.* **2006**, *71*, 6178. (b) Fernández, I.; Cossío, F. P.; Sierra, M. A. *J. Org. Chem.* **2007**, *72*, 1488. (c) Fernández, I.; Sierra, M. A.; Cossío, F. P. *J. Org. Chem.* **2008**, *73*, 2083, and references therein. (26) (a) Foster, J. P.; Weinhold, F. *J. Am. Chem. Soc.* **1980**, *102*, 7211. (b) Reed, A. E.; Weinhold, F. *J. Chem. Phys.* **1985**, *83*, 1736. (c) Reed, A. E.; Weinstock, R. B.; Weinhold, F. *J. Chem. Phys.* **1985**, *83*, 735. (d) Reed, A. E.; Curtiss, L. A.; Weinhold, F. *Chem. Rev.* **1988**, *88*, 899.

energies associated with the two-electron interactions have been computed according to the following equation:

$$\Delta E_{\phi\phi^*}^{(2)} = -n_{\phi} \frac{\langle \phi^* | \hat{F} | \phi \rangle^2}{\varepsilon_{\phi^*} - \varepsilon_{\phi}}$$

where  $\hat{F}$  is the DFT equivalent of the Fock operator and  $\phi$  and  $\phi^*$  are two filled and unfilled Natural Bond Orbitals having  $\varepsilon_{\phi}$  and  $\varepsilon_{\phi^*}$  energies, respectively;  $n_{\phi}$  stands for the occupation number of the filled orbital.

Solvents were dried by standard methods and distilled under argon. Tetrafluoroboric acid diethyl ether complex was obtained from Aldrich and used as received. 1,2-diphenyl-3,5-dichloropyrazolium tetrafluoroborate was prepared using modified literature procedures as outlined in the Supporting Information.

**1,2-Diphenyl-3,5-bis(dimethylamino)pyrazolium<sup>12</sup> Tetrafluoroborate (2 g-BF<sub>4</sub>).** A 20 mL chloroform suspension of 1,2-diphenyl-3,5-dichloropyrazolium<sup>27</sup> tetrafluoroborate (1.0 g, 2.65 mmol) was cooled to  $-78$  °C under argon. A large excess of dimethylamine was condensed in the flask. The reaction was stirred for 1 h at low temperature, then let to come to room temperature and stirred for an additional 2 h. The solution was concentrated under vacuum and diethylether was added to precipitate a tan solid. The solid was washed with water  $4 \times 50$  mL and diethylether  $2 \times 50$  mL. Drying gave 735 mg (1.86 mmol) of a light-tan solid (70% yield). Mp. 210 °C; <sup>1</sup>H NMR (CDCl<sub>3</sub>, 300 MHz):  $\delta$  2.87 (s, 12H), 5.61 (s, 1H), 6.94 (d, 4H), 7.36–7.48 (m, 6H); <sup>13</sup>C NMR (CDCl<sub>3</sub>, 75 MHz):  $\delta$  41.6 (CH<sub>3</sub>), 78.5 (CH), 128.3 (C<sub>Ar</sub>H), 130.3 (C<sub>Ar</sub>H), 130.8 (C<sub>Ar</sub>H), 138.8 (C<sub>Ar</sub>), 164.8 (NCN). Single crystals were grown from a hot concentrated methanol solution, by slow cooling to  $-20$  °C.

**1,2-Diphenyl-3,5-bis(dimethylamino)-4H-pyrazole-1,2-diium Bis(tetrafluoroborate) (2 g-2BF<sub>4</sub>).** Tetrafluoroboric acid diethyl ether complex (0.076 mL, 0.558 mmol) was added dropwise to a solution of **2g**-BF<sub>4</sub> (0.200 g, 0.507 mmol) in 2 mL of CH<sub>3</sub>CN at room temperature. <sup>13</sup>C NMR of the reaction mixture shows a complete and quantitative reaction within two minutes. Crystals of **3g**-2BF<sub>4</sub>, suitable for an X-ray diffraction analysis, were obtained by slow diffusion of ether vapor in the reaction mixture at  $-20$  °C. After washing with ether, and drying in vacuo, 0.20 g (0.415 mmol, 82%) of colorless **3g**-2BF<sub>4</sub> was obtained. Mp. 216–217 °C with decomposition (decomp begins at 200 °C); Dissolving crystals of **3g**-2BF<sub>4</sub> in acetonitrile-d<sub>3</sub> result in a 7:3 mixture of **3g**-2BF<sub>4</sub> and **2g**-BF<sub>4</sub> along with free HBF<sub>4</sub>. <sup>1</sup>H NMR for **3g**-2BF<sub>4</sub> (CD<sub>3</sub>CN, 300 MHz):  $\delta$  2.68 (s, 6H), 3.40 (s, 6H), 4.98 (s, 2H), 7.35–7.51 (m, 10H); <sup>13</sup>C NMR (CD<sub>3</sub>CN, 75 MHz):  $\delta$  42.2 (CH<sub>3</sub>), 43.3 (CH<sub>2</sub>), 46.2 (CH<sub>3</sub>), 131.1 (C<sub>Ar</sub>H), 132.7 (C<sub>Ar</sub>H), 133.0 (C<sub>Ar</sub>), 134.1 (C<sub>Ar</sub>H), 158.8 (NCN). Peaks are also observed for HBF<sub>4</sub> (br s, 9.11 ppm in <sup>1</sup>H NMR) and for 30% of **2g**-BF<sub>4</sub>: <sup>1</sup>H NMR (CD<sub>3</sub>CN, 300 MHz):  $\delta$  2.81 (s, 12H), 5.49 (s, 1H), 7.00–7.03 (m, 4H), 7.37–7.47 (m, 6H); <sup>13</sup>C NMR (CD<sub>3</sub>CN, 75 MHz):  $\delta$  41.9 (CH<sub>3</sub>), 78.9 (CH), 129.6 (C<sub>Ar</sub>H), 131.0 (C<sub>Ar</sub>H), 131.6 (C<sub>Ar</sub>H), 139.2 (C<sub>Ar</sub>), 164.9 (NCN).

**Acknowledgment.** This work was supported by the NSF (CHE 0808825), NSERC (postdoctoral fellowship for C.A.D.) and the Deutsche Forschungsgemeinschaft. I.F. is a Ramón y Cajal fellow. We express our gratitude to Dr. Carlos Silva for his assistance with the ACID plot.

**Supporting Information Available:** Experimental procedures, Cartesian coordinates (in Å), and total energies of all the stationary points discussed in the text, crystallographic information files (CIF), and complete ref 18. This material is available free of charge via the Internet at <http://pubs.acs.org>.

JA903396E

(27) Kira, M. A.; Ghaleb, H. A.; Shoeb, H. A.; Osman, A. I.; Mansy, F. *U. A. R. J. Chem.* **1970**, *13*, 513–517.